NASA/CR-2007-214859

An Analysis of the Effects of RFID Tags on Narrowband Navigation and Communication Receivers

E. F. Charles LaBerge
Honeywell Research and Technology Center, Columbia, Maryland

March 2007

The NASA STI Program Office . . . in Profile

Since its founding, NASA has been dedicated to the advancement of aeronautics and space science. The NASA Scientific and Technical Information (STI) Program Office plays a key part in helping NASA maintain this important role.

The NASA STI Program Office is operated by Langley Research Center, the lead center for NASA's scientific and technical information. The NASA STI Program Office provides access to the NASA STI Database, the largest collection of aeronautical and space science STI in the world. The Program Office is also NASA's institutional mechanism for disseminating the results of its research and development activities. These results are published by NASA in the NASA STI Report Series, which includes the following report types:

- TECHNICAL PUBLICATION. Reports of completed research or a major significant phase of research that present the results of NASA programs and include extensive data or theoretical analysis. Includes compilations of significant scientific and technical data and information deemed to be of continuing reference value. NASA counterpart of peer-reviewed formal professional papers, but having less stringent limitations on manuscript length and extent of graphic presentations.

- TECHNICAL MEMORANDUM. Scientific and technical findings that are preliminary or of specialized interest, e.g., quick release reports, working papers, and bibliographies that contain minimal annotation. Does not contain extensive analysis.

- CONTRACTOR REPORT. Scientific and technical findings by NASA-sponsored contractors and grantees.

- CONFERENCE PUBLICATION. Collected papers from scientific and technical conferences, symposia, seminars, or other meetings sponsored or co-sponsored by NASA.

- SPECIAL PUBLICATION. Scientific, technical, or historical information from NASA programs, projects, and missions, often concerned with subjects having substantial public interest.

- TECHNICAL TRANSLATION. English-language translations of foreign scientific and technical material pertinent to NASA's mission.

Specialized services that complement the STI Program Office's diverse offerings include creating custom thesauri, building customized databases, organizing and publishing research results ... even providing videos.

For more information about the NASA STI Program Office, see the following:

- Access the NASA STI Program Home Page at ***http://www.sti.nasa.gov***

- E-mail your question via the Internet to help@sti.nasa.gov

- Fax your question to the NASA STI Help Desk at (301) 621-0134

- Phone the NASA STI Help Desk at (301) 621-0390

- Write to:
  NASA STI Help Desk
  NASA Center for AeroSpace Information
  7115 Standard Drive
  Hanover, MD 21076-1320

NASA/CR-2007-214859

An Analysis of the Effects of RFID Tags on Narrowband Navigation and Communication Receivers

E. F. Charles LaBerge
Honeywell Research and Technology Center, Columbia, Maryland

National Aeronautics and
Space Administration

Langley Research Center
Hampton, Virginia 23681-2199

Prepared for Langley Research Center
under Purchase Order NNL06AC06P

March 2007

Acknowledgments

This work was funded by the Federal Aviation Administration as part of FAA/NASA Interagency Agreement DFTA03-96-X-90001, Revision 9, as well as the NASA Aviation Safety Program (Single Aircraft Accident Prevention Project).

Available from:

NASA Center for AeroSpace Information (CASI)
7115 Standard Drive
Hanover, MD 21076-1320
(301) 621-0390

National Technical Information Service (NTIS)
5285 Port Royal Road
Springfield, VA 22161-2171
(703) 605-6000

ABSTRACT

The simulated effects of the Radio Frequency Identification (RFID) tag emissions on ILS Localizer and ILS Glide Slope functions match the analytical models developed in support of DO-294B provided that the measured peak power levels are adjusted for 1) peak-to-average power ratio, 2) effective duty cycle, and 3) spectrum analyzer measurement bandwidth. When these adjustments are made, simulated and theoretical results are in extraordinarily good agreement. The relationships hold over a large range of potential interference-to-desired signal power ratios, provided that the adjusted interference power is significantly higher than the sum of the receiver noise floor and the noise-like contributions of all other interference sources. When the duty-factor adjusted power spectral densities are applied in the evaluation process described in Section 6 of DO-294B , most narrowband guidance and communications radios performance parameters are unaffected by moderate levels of RFID interference. Specific conclusions and recommendations are provided.

1 INTRODUCTION

A recent NASA study [1] investigates the emissions of various classes of RF[1] identification tags (RFID tags or RFIDs) in frequency bands associated with radios that are commonly installed on aircraft to perform communications, navigation and surveillance functions. Although the emissions are generally of low level, [1] reports measured emissions of one particular tag type that appear to be unacceptably high in the 328.6-335.4 MHz band associated with the Instrument Landing System (ILS) Glide Slope (GS) function [2, 3]. NASA Langley Research Center awarded a small study contract to Honeywell to investigate the potential impact of such interference on GS operations, and to recommend appropriate modifications to the susceptibility levels reported in DO-294B [4] . This report contains the analysis, supporting simulations, and the requested recommendations. In addition, this note extends the analysis to provide relatively simple relationships that will be useful to estimate the effects of RFID or other bursty emissions on narrowband communication, navigation and surveillance receivers, such as Localizer (LOC), Very High Frequency Omnirange (VOR), Marker Beacon, and Very High Frequency (VHF) voice communications. The analysis and simulations were performed at the Honeywell's Navigation, Communication and Control Systems Research and Technology Center in Columbia, MD.

1.1 Executive Summary

The effect of the gated radio frequency (RF) noise emissions measured by [1] match the analytical models developed in support of DO-294B provided that the measured peak power levels are adjusted for 1) peak-to-average power ratio, 2) effective duty cycle, and 3) spectrum analyzer measurement bandwidth. When these adjustments are made, simulated and theoretical results are in extraordinarily good agreement.

The relationships hold over a large range of potential interference-to-desired signal power ratios, provided that the adjusted interference power is significantly higher than the sum of the receiver noise floor and the noise-like contributions of all other interference sources.

For the particular Mantis RFID tags reported on by [1], there appears to be a significant difference between the emission levels measured in [1] and those reported in the Federal Communications Commission (FCC) compliance testing. The levels reported in [1] significantly

[1] A table of acronyms and abbreviations is provided in Appendix A.

exceed the permissible emissions required under 47CFR15. This is almost certainly due to the difference in measurement practices. Part 15 [5] requires the use of a quasi-peak detector, while the equivalent aviation standard, DO-160 [6] uses a peak detector. The output of the quasi-peak detector is reduced with lower duty cycle, whereas the peak detector output is not. The results reported in [1] were made using the peak detector method, and therefore are *pessimistic* with respect to the actual effect on the victim radios.

1.2 Conclusions

Section 6 reports five conclusions based on the analysis and simulation efforts described in this report. In summary form, these conclusions are:

1. The effect of low-duty cycle RFID tags on the guidance output of the narrowband navigation system (GS, LOC, VOR) is proportional to the effective duty cycle of the transmissions and inversely proportion to the carrier to interference ratio at the receiver input, as measured during the duration of a single pulse.

2. Simulations of generic ILS receiver processing confirm the form of (13) for pulsed noise-like interference.

3. When the effective average interference levels predicted by (13) are used, the *pro forma* analysis recommended by Section 6 DO-294B indicates that the effects of RFID emissions ILS GS are probably negligible on large cargo aircraft.

4. When the effective average interference levels predicted by (13) are used, the *pro forma* analysis recommended by Section 6 DO-294B indicates that the effects of RFID emissions ILS LOC and VOR receivers should be negligible across a wide range of aircraft, duty cycle, and multiple equipment factor considerations.

5. When single-pulse interference levels are considered, a preliminary evaluation of the susceptibility of VHF voice and data receivers indicates that the effects of relatively low-power (5 dBm) RFID tags on those VHF communications systems should be negligible.

1.3 Recommendations

Section 7 makes five recommendations regarding further work related to this report. In summary form, these recommendations are:

1. Additional cargo-bay measurements of interference path loss (IPL) in both the frequency band of intentional emissions of the RFID device(s) and the frequency band of the desired avionics signal(s) should be conducted on large cargo aircraft, especially in the GS band. These measurements will serve to validate several assumptions made in the analysis sections of this report.

2. The models used here consider a pulsed-noise form of interference from the RFID tags. These results should be extended to consider pulsed-CW forms of interference.

The limited scope of effort for the tasks reported here was focused on the effects of RFID tags on narrowband guidance systems, including ILS Localizer, ILS GS and VOR. Nevertheless a preliminary analysis of other VHF systems was conducted. The following recommendations cover this preliminary analysis

3. Additional analysis of VHF voice susceptibility to the pulsed interference from RFID tags should be considered, with specific emphasis on the spurious susceptibility of the victim receiver.

4. Additional analysis of VHF data digital data susceptibility to the pulsed interference from RFID tags should be considered, with specific emphasis on the spurious susceptibility of the victim receiver.

This study effort was limited to narrowband VHF /UHF receivers. While these are expected to be the most susceptible to RFID emissions, there are many other systems that have not been analyzed.

5. An analysis similar to that reported here should be considered for the remaining systems listed in Table 6-2 of DO-294B.

2 SUMMARY DESCRIPTION OF WAVEFORMS USED IN THE ANALYSIS

2.1 Glide Slope

The Instrument Landing System (ILS) is a precision approach and landing system approved by ICAO for use in Category III, zero-visibility landings. Lateral and precision vertical guidance in ILS are provided by means of the Localizer (LOC) and Glide Slope (GS) functions, respectively. Both functions use simple double-sideband amplitude modulation (DSB-AM) to encode the guidance signals, albeit with slightly different modulation parameters. The LOC operates on channels in the 108.1-111.95 MHz band; GS operates in the 328.6-335.4 MHz band. In both cases, the guidance signal consists of amplitude modulation with a composite of 90 Hz and 150 Hz tones. The aircraft is determined to be on course if the receiver measures the depth of modulation of the two tones to be equal. Predominance of one tone over the other leads to either "fly left/fly right" or "fly up/fly down" indications to the pilot or automatic flight control system, depending on whether the guidance function is LOC or GS, respectively.

Consider an on-course LOC or GS signal with a depth of modulation (i.e., modulation index) of $m_{90} = m_{150} = m$. The time waveform is given by

$$v(t) = A\left(1 + m\sin(2\pi 90t) + m\sin(2\pi 150t)\right)\cos(\omega_c t + \phi), \tag{1}$$

where A is the (voltage) amplitude of the signal, ω_c is the radian frequency of the RF carrier and ϕ is the arbitrary carrier phase at the instant $t = 0$. A noise-free ILS GS waveform is shown in Figure 1, where the time scale is too long to show individual cycles of the carrier.[2]

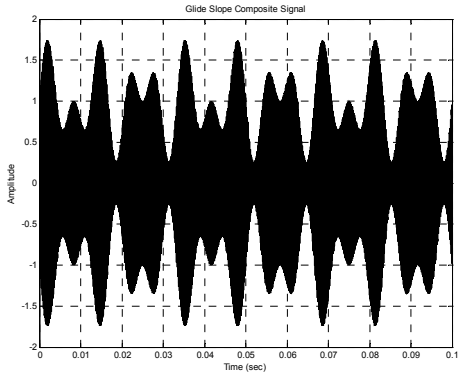

Figure 1 Ideal On-Course GS Signal

For convenience, and without loss of generality, we choose the time origin to be at an instant where the voltage envelope achieves its maximum value of $v_{\max} = A(1+2m)$. All basic texts in communication systems engineering (see, [7], for example) give the two-sided voltage spectrum of the voltage waveform in (1) as the sum of ten terms,

[2] For the purpose of simulation and illustration in the this report, a carrier frequency of approximately 125 kHz is used in lieu of the actual 300 MHz GS carrier. Because this frequency is much larger than either modulation frequency, use of such simplifications does not affect the analysis or simulation results.

$$V(f)=\frac{Am}{4}\left(\begin{array}{l}\delta(f-\frac{\omega_C}{2\pi}-150)+\delta(f-\frac{\omega_C}{2\pi}-90)+\delta(f-\frac{\omega_C}{2\pi}+90)+\delta(f-\frac{\omega_C}{2\pi}+150)\\ -\delta(f+\frac{\omega_C}{2\pi}-150)-\delta(f+\frac{\omega_C}{2\pi}-90)-\delta(f+\frac{\omega_C}{2\pi}+90)-\delta(f+\frac{\omega_C}{2\pi}+150)\end{array}\right) \quad (2)$$
$$+\frac{A}{2}\left(\delta(f-\frac{\omega_C}{2\pi})-\delta(f+\frac{\omega_C}{2\pi})\right)$$

where $\delta(x)$ is the Dirac delta function. The generalize voltage spectrum, $V(f)$ for $m_{90}\neq m_{150}$ is shown in Figure 2.

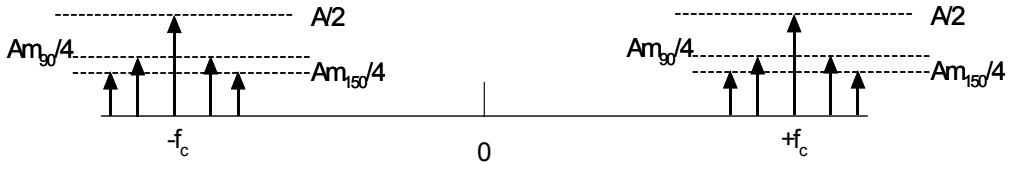

Figure 2 Voltage Magnitude Spectrum *V(f)* of an Ideal ILS Guidance Signal

The sum of the magnitudes of the ten voltage components gives the maximum envelope voltage

$$\begin{aligned}v_{\max}&=\frac{Am}{4}(1+1+1+1+1+1+1+1+1+1)+\frac{A}{2}(1+1)\\&=\frac{8Am}{4}+\frac{2A}{2}\\&=A(1+2m)\end{aligned} \quad (3)$$

Similarly, the absolute depth of modulation of the 90 Hz component is obtained by summing the amplitudes of the voltage spectrum of the four sidebands associated with frequencies of $\pm\frac{\omega_C}{2\pi}\pm 90$ Hz,

$$d_{90}=\frac{Am}{4}(1+1+1+1)=Am \quad (4)$$

The 150 Hz component is similarly obtained,

$$\begin{aligned}d_{150}&=\frac{Am}{4}(1+1+1+1)\\&=Am\end{aligned} \quad (5)$$

ILS guidance is linearly proportional to the *difference in the depth of modulation* (ddm) expressed as a normalized fraction of the carrier amplitude, that is, to the *normalized amplitude* of the modulating sinusoids. For the 90 and 150 Hz components, the absolute amplitude is given by summing the amplitudes of the constituent frequency components, as given in (4) and (5). The guidance signal is thus

$$ddm(t)=\frac{Am_{90}-Am_{150}}{A}=m_{90}-m_{150} \quad (6)$$

The guidance signal, $ddm(t)$ is a function of time only because of aircraft motion about the desired approach path. The values of the modulation indices, m_{90} and m_{150} are constants that are established in the relevant standards for LOC and GS.

For the GS case, [3] states that the receiver centering error shall not exceed "13% of standard deflection". With standard deflection of 0.091 [3, 2.4.1.j]

$$0.13 \times 0.091 \text{ ddm} = 0.0118 \text{ ddm}^{3} \tag{7}$$

As a practical matter, the bandwidth of the ILS measurement is limited to a small, but non-zero, bandwidth. Some small bandwidth is necessary to permit the receiver to track aircraft movements about the desired path. Reducing the equivalent lowpass processing bandwidth below approximately 0.5 Hz renders the receiver output incapable to responding to aircraft motion and thus unusable as a guidance signal. [For an excellent discussion of output signal bandwidth in guidance receivers, see 8]

Consider the ideal case, where perfect bandpass filters with bandwidth B Hz could be designed at the frequencies $\frac{\omega_C}{2\pi} \pm 90$ Hz and $\pm\frac{\omega_C}{2\pi} \pm 150$. If there were no noise present on the signal, the response of these filters would be the desired voltage magnitude from (2), as shown in Figure 2.

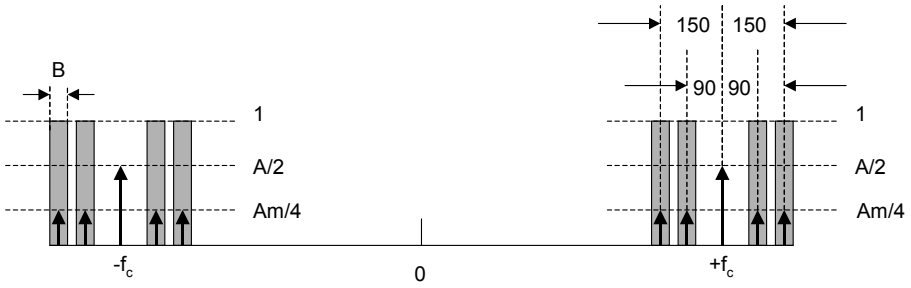

Figure 3 ILS with Idealized Bandpass Filters

Both LOC [9] and GS [3] MOPS specify a low-pass filter equivalent to an ideal noise bandwidth of approximate 0.46 Hz. This corresponds to an idealized IF bandpass bandwidth, *B*, of 0.92 Hz. While it is useful to consider such an idealized frequency in the analysis conducted below, it is obviously impractical to construct such filters for use in real receivers.[4] Real receivers are constructed in a classical super heterodyne architecture, with a series of down conversions, filters, and envelope detectors. This architecture is used even when the bulk of the signal processing is performed digitally, as is done in virtually all modern receivers. Nevertheless, for the purpose of this analysis and other similar contemporaneous analyses [10-12] use the equivalent idealized narrow-band IF bandwidth as a key element in the analysis.[5]

[3] Although we will continue to use the "unit" of "ddm", in fact, the computations of (6) and (7) have units Volts/Volt, and are, therefore, essentially unitless.

[4] Such a filter would have a filter quality factor of $Q > 10^8$!

[5] The analysis provided here for the noise-only case is not a strict quantitative analysis. Several different quantitative analyses of the entire idealized-receiver case all obtain the same 2/CNR result.

2.2 Mantis RFID

Like many other RFID products, the Mantis RF tag uses a proprietary waveform and protocol. Based on [1], when measured with a peak detector, the Mantis tag has significant emissions within the GS band. An example of a measured "zero span", i.e., time domain, power measurement of a single pulse within the Mantis format is shown in Figure 4. An individual pulse is approximately 10 microseconds in duration. The measurement is within a 1 MHz bandwidth centered at 333.9 MHz.

The Mantis signal format appears to consist of a series of bursts of approximately 112 ms in duration, as shown in Figure 5. There are approximately 70 pulses spaced 1.6 ms apart in a Pulse Amplitude Modulation (PAM) or On-Off Keying (OOK) scheme. The pulse pattern is constant for a given RFID tag. The bursts occur as close together as 600 ms, although the standard spacing can be programmed to larger values.

The GS band (328.6-336.4 MHz) is well separated from the Mantis tag transmission frequency (303.8 MHz). The separation is sufficient to assure that the spectrum from the PAM modulation is down at least 60 dB from the on-channel signal. Therefore, the residual pulse-like signal within the GS band is either noiselike in nature or due to a narrowband spurious signal generated by the Mantis device.

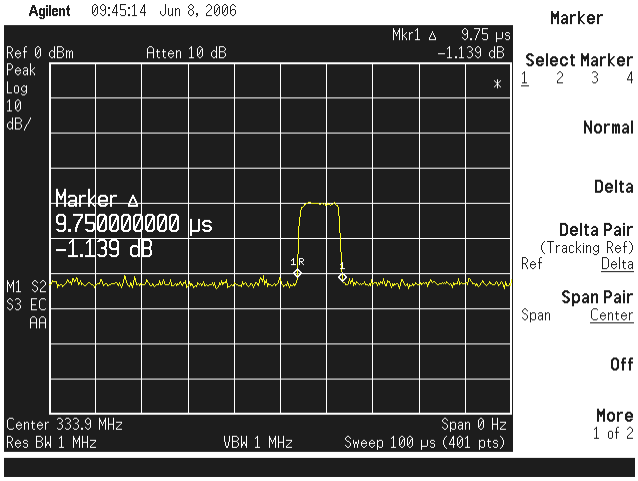

Figure 4 "Zero Span" Mantis Signal on GS Channel, Single Pulse

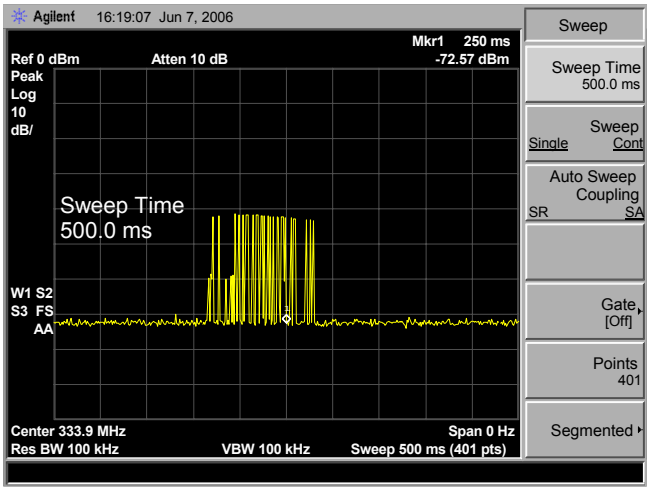

Figure 5 "Zero Span" Mantis Signal on GS Channel, Sub burst

3 ANALYSIS

3.1 Summary of ILS Analysis

The simplest analysis of the GS accuracy [6] is to recognize that the guidance signal *ddm* given by (6) is obtained by (coherent) voltage summation of the outputs of the four relevant filters at 90 Hz and the four relevant filters at 150 Hz, subtracting the results and normalizing by the amplitude *A*. As shown above, the result is the depth of modulation. Noise errors in the estimate of the carrier amplitude cause second order effects, which can be made small by proper choice of the carrier estimation bandwidth[7], and are ignored in this simple analysis.

Now consider the effect of additive white Gaussian noise (AWGN) of two-sided power spectral density $\frac{N_0}{2}$ watts/Hz. Because the bandwidth B must be wide enough to accommodate parameter variations in the guidance, there will be a small amount of noise power present on even an ideally detected signal. The total noise power in this measurement is the total noise power in the eight bands of the two-sided spectrum shown in Figure 3. Because the filters are idealized, the noise power in each of the eight filter bands in Figure 3 is $N = \frac{N_0 B}{2}$, thus the total noise power in the filters centered on all of the sidebands is

$$N_{TOTAL} = 8 \times \frac{N_0 B}{2} = 4 N_0 B \text{ Watts.} \tag{8}$$

If we assume zero mean noise, and an on-course guidance signal, we can show that the variance in the measurement is the total noise power, N_{TOTAL}, divided by the square of the normalizing factor, A^2,

[6] This GS analysis is identical to that presented in [7] for Localizer.
[7] Unlike the guidance signal (i.e., the 90 Hz and 150 Hz modulation signals) the *carrier* measurement bandwidth does not directly affect the ability of the receiver to track aircraft motion. Again, see [8].

$$\mathrm{Var}[ddm] = \sigma_{ddm}^2 = \frac{4N_0B}{A^2} = \frac{2}{\frac{A^2}{2}\times\frac{1}{N_0B}} = \frac{2}{CNR} \tag{9}$$

where the *CNR* is measured in a bandwidth of *B* Hz. Note that this expression uses the *carrier* amplitude and not the *sideband* amplitude as a point of reference. This is appropriate, as ILS sensitivity in [3, 9] is specified in terms of the *carrier* level, not the sideband levels.

3.2 Generic Noise-like Pulsed Interference Analysis

The result given in (9) applies when the receiver is continuously subjected to broadband noise or broadband interference.[8] When the noise level is due to an interference source that is bursty or pulse-like in nature, it is natural to suspect that the long term average effects, including both the mean and standard deviation of the guidance error, will vary with the duty cycle, η, of the pulse/burst phenomenon. If the operating frequency of the interference source is sufficiently separated from the victim receiver frequency that the *signal structure* of the interference is negligible, then the effects appear at the receiver input as gated noise with a duty cycle of η, and it is reasonable to assume that the gating function, $g(t)$, and the noise function, $n(t)$, are *independent*. We can treat the gating function $g(t)$ as a binary random process where $g(t)=1$ means that the RFID is transmitting at time t and $g(t)=0$ implies that it is not transmitting. We can then describe the probability density function of $g(t)$ as

$$p_g(g) = \begin{cases} \eta \text{ for } g(t)=1 \\ (1-\eta) \text{ for } g(t)=0 \\ 0 \text{ otherwise} \end{cases} \tag{10}$$

We assume that the noise is a zero-mean Gaussian process with $I=\sigma^2$, where I is the interference measured at the receiver input in an appropriate bandwidth.

By assuming that the random processes $g(t)$ and $n(t)$ are independent, we naturally have that they are also uncorrelated. Therefore, if we define the (random) interference as $i(t)=g(t)n(t)$ we have that

$$E[i(t)] = E[g(t)n(t)] = E[g(t)]E[n(t)] = 0 \tag{11}$$

and

$$\begin{aligned} \mathrm{var}[i(t)] &= \sigma_i^2 = E\left[i^2(t)\right] = E\left[g^2(t)\right]E\left[n^2(t)\right] \\ &= 1^2\times\eta\times\sigma^2 + 0^2\times(1-\eta)\times\sigma^2 = \eta\sigma^2 \end{aligned} \tag{12}$$

Substituting (12) into (9) we can write an approximation for the variance in the guidance signal due to gated noise-like interference generated by a pulsed transmitter as

[8] In this case, the term "broadband" means "the power spectral density of the noise is sufficiently wide to affect all of the modulation bands at essentially the same level".

$$\sigma_{ddm}^2 = \frac{4\eta I_0 B}{A^2} = \frac{2\eta}{CIR} = 2\eta\rho^2 \tag{13}$$

where I_0 is the Power Spectral Density (PSD) of the interference "noise" before gating, *CIR* is the carrier power-to-interference power ratio. We define $\rho^2 = 1/CIR = 2\sigma^2/A^2$ as the interference-to-carrier power ratio. Equation (13) is satisfying from an intuitive point of view, as it predicts that the guidance error will *increase* as the interference power increases (i.e., as ρ^2 gets larger) and will *decrease* as the duty cycle of the interfering bursts gets smaller.

3.3 Application to Mantis RFID tags

To apply the theory of the previous section to Mantis RFID tags, we need to verify that the amplitude of any modulation-related spectrum structure is negligible. If this is true, we will be justified in our use of gated-noise approximation as the unwanted emissions. The NASA measurements reported in [1] suggest single-source emissions in the range of -20 dBm. At the same time, the reported maximum intentional transmit power is 5 mw (+7 dBm). Given the rectangular pulse gating function shown in Figure 4, with the resulting $\sin^2 \pi\Delta fT/(\pi\Delta fT)^2$ power spectrum, the modulated spectrum structure at $\Delta f = 30$ MHz should be down by $20\log_{10}(\pi\Delta fT) = 60$ dB relative to the maximum intentional power, or -53 dBm. Thus, the modulated signal-structure is approximately 30 dB below the unintentional emissions. Therefore, we can ignore the modulated signal structure component and concentrate on noise-like spurious emissions.

The second constraint is that the interference gating function is independent of the interference noise. While this is less obviously true, it is reasonable to assume that the spurious noise emitted during periods of intentional transmission is not related to the time or duration of the intentional emissions.

For the Mantis tags specifically considered in this report, the value of the transmission duty factor[9] η is given by the product of several factors

$$\begin{aligned}\eta &= \frac{\text{duration of single pulse}}{\text{pulse repetition interval}} \times \frac{\text{Number of pulse slots per burst} \times \text{pulse repetition interval}}{\text{Burst duration}} \\ &\quad \times \frac{\text{Burst duration}}{\text{Burst Repetition Interval}} \times \Pr\{\text{Pulse is transmitted}\} \\ &= \frac{t_p}{T_p} \times \frac{N_p T_p}{t_{burst}} \times \frac{t_{burst}}{T_{burst}} \times \Pr\{1\} = \frac{N_p t_p p_1}{T_{burst}}\end{aligned} \tag{14}$$

Additionally, the power spectral density of the emissions must be reduced to an 0.92 Hz bandwidth so that (13) can be used to estimate the guidance variance induced by the Mantis tag. With a Mantis pulse shown in Figure 4, $t_p \approx 10\ \mu$sec, and the idealized $\sin^2 \pi\Delta fT/(\pi\Delta fT)^2$ power spectrum has a width of 100 kHz >> 1 Hz. Therefore, the emissions appear to be white noise with respect to the guidance signal. The measured PSD should be *reduced* by the ratio of the

[9] We will use the terms "transmission duty factor", "duty cycle" and "efficiency factor" interchangeably throughout this document.

spectrum analyzer measurement bandwidth to the idealized ILS guidance IF bandwidth of 0.92 Hz. For convenience, we will also consider this factor to be part of the efficiency factor, η

$$\eta = \frac{N_p t_p p_1}{T_{burst}} \times \frac{B_{ILS}}{B_{SA}} = \frac{N_p t_p p_1 B_{ILS}}{T_{burst} B_{SA}} \tag{15}$$

4 SIMULATION

A simulation of generic ILS signal processing was used to verify these analytical models. The intent of this simulation effort was to model a generic, nearly ideal, GS receiver. The simulation specifically *did not* model any particular GS implementation. Instead, the focus was on features common to all ILS receiver implementations.

4.1 Summary of ILS Simulation

The simulation of the ILS signal processing was developed in MATLAB using both standard and customized MATLAB functions. The simulation provides a means to examine the signal resulting at each step in the process. Representative outputs are provided in Appendix B.

Figure 6 shows a block diagram of the simulation model. Blocks 1, 2, and 3 generate a composite GS, RFID, and noise signal as the input to the receiver model. A real (as opposed to complex) signal model is used, that is, the desired GS signal in Block 1 is given by (1). Without loss of generality, the RF phase, ϕ, is assumed to be zero.[10] For simulation reasons, a carrier frequency of approximately 125 kHz and a sample frequency of 500 ksps are used. An on-course GS signal with $m_{90} = m_{150} = 0.4$ is used for all of the analysis.

Within the receiver simulation, a 40 kHz IF bandpass filter is modeled (Block 4), using the MATLAB Butterworth filter routine. In Block 5, an ideal synchronous detector routine generates the envelope of the composite RF signal. For simulation reasons, the signal is downsampled to 4000 ksps (Block 6). This detected envelope feeds parallel 90 Hz and 150 Hz processing paths. Each path consists of an appropriate bandpass filter (Blocks 7a and 7b) and another idealized synchronous detector (Blocks 8a and 8b). The outputs of the synchronous detectors (Blocks 8a and 8b) are the estimated levels of the 90 Hz and 150 Hz tones. These values are subtracted to generate the guidance signal $\widehat{ddm}$. For simulation reasons, the guidance estimate is downsampled to 100 sps (Block 9) and then filtered through a single-pole low-pass filter satisfying the constraints of [3] (Block 10). The output of the receiver model is then used to accumulate the statistics for future analysis (Block 11).

Each trial of the simulation generates a composite signal record that is 5 seconds long, corresponding to 2.5 million samples of the simulated RF signal. To accumulate stable statistics, two hundred trials are performed at each combination (CNR, ρ^2). To account for the transient response of the tone detection filters (Blocks 7a and 7b) and the output low-pass filter (Block 10), the first two seconds of each simulation record are discarded.

[10] This assumption involves no loss in generality because the carrier frequency is much greater than the maximum modulation frequency of 150 Hz and because RF phase carries no information in ILS in general, and GS in particular.

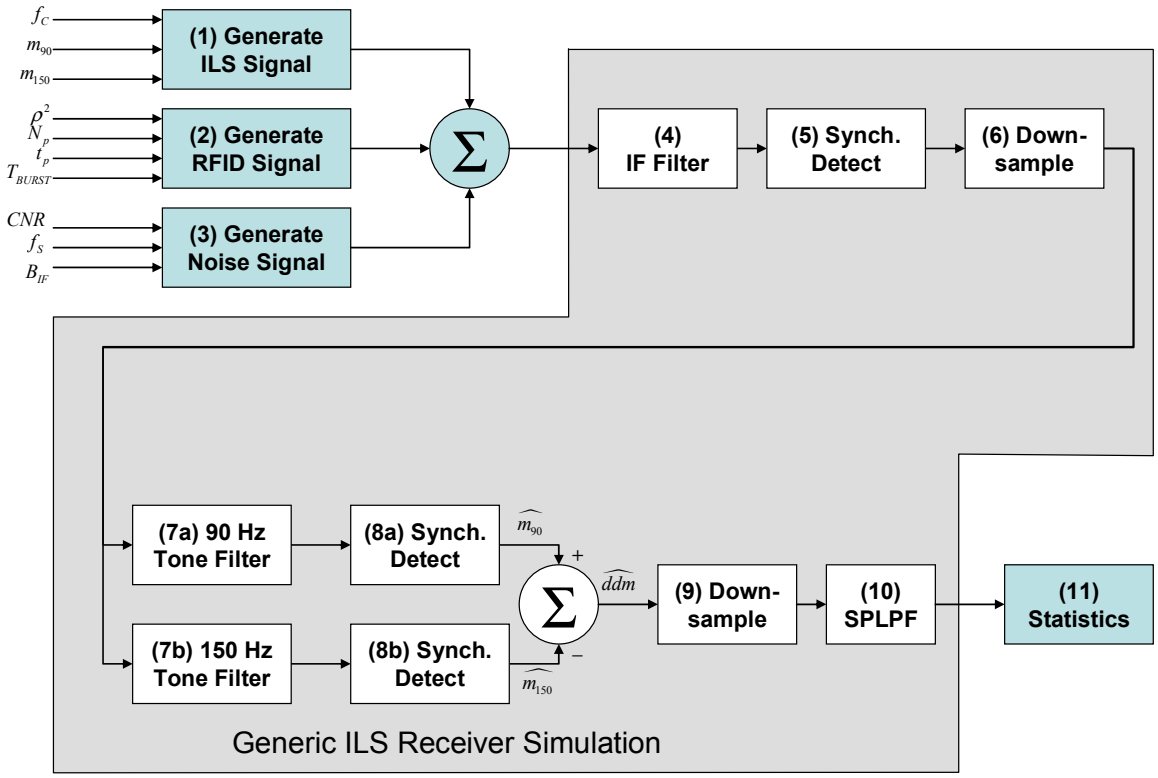

Figure 6 Block diagram of generic ILS receiver simulation

Representative waveforms and spectra at the various points in the simulation are contained in Appendix B to this report.

4.2 Noise Only Results

To validate the simulation, a series of experiments was performed with the interference-to-desired signal voltage ratio, ρ, set to zero. Ideally, this should reproduce a curve with the shape indicated by (9). Two sets of statistics were collected from the simulated data. First, the mean of the last three seconds of data collected from each trial was computed. A "variance of means" statistic was then computed over the $N = 200$ trial ensemble. If $\overline{x}_k$ is the mean value of the *k*-th trial, this "variance of means" (VoM) statistic is given by

$$VoM = \sigma_{\overline{x}}^2 = \frac{1}{N}\sum_{k=1}^{N}(\overline{x}_k)^2 - \left(\frac{1}{N}\sum_{k=1}^{N}\overline{x}_k\right)^2 \tag{16}$$

The same data was used to compute a "mean of variances" (MoV) statistic from the variances of the individual trials, σ_k^2:

$$MoV = \overline{\sigma_x^2} = \frac{1}{N}\sum_{k=1}^{N}\sigma_k^2 \tag{17}$$

At each of the CNR values simulated, the approximate relationship

$$MoV \approx 2 \times VoM \tag{18}$$

was observed. We believe this to be a function of both the length of the time record collected for each observation and the duration of the "transient rejection" period at the start of each time record. This discrepancy could not be resolved in the time allotted this investigation.

Figure 7 shows that the simulated VoM closely approximates the $2/CNR$ curve predicted from the theory. Therefore, the VoM statistic was used in the remainder of the analysis.

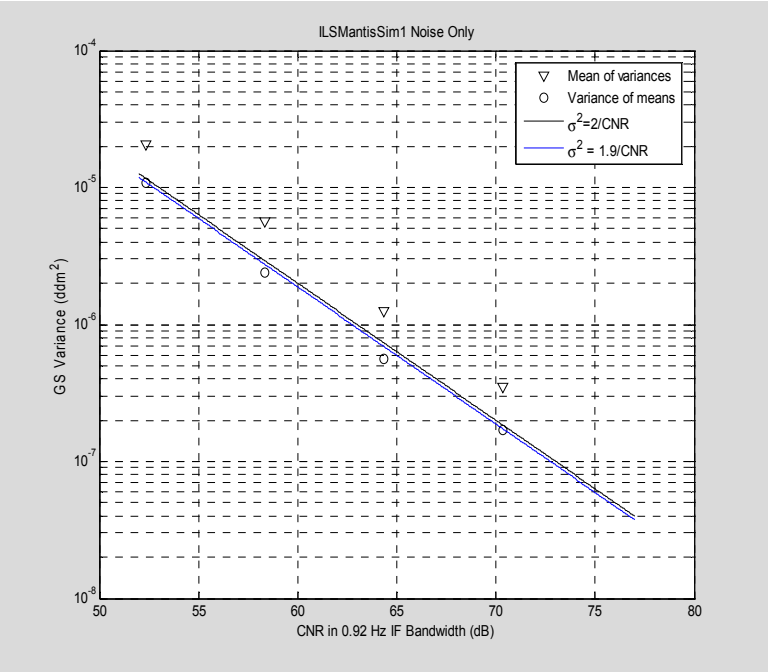

Figure 7 Noise-only simulation results vs. theory

4.3 Comparison of Simulation with Analysis

With the model validated for the noise-only case, the Mantis RFID interference was added in a parametric way. For the purpose of this study, the parameter of choice was the transmission duty factor, η, defined in (14). $N = 200$ simulation trials were run for each combination of (CNR, ρ^2) and the VoM statistics accumulated according to (16). The results were then plotted for comparison with the relationship given by (13). The various value of η were obtained by different combinations of t_p, N_p and T_{burst}. For all trials $p_0 = p_1 = 0.5$, i.e., the random data within the ID was assumed to have equally probable 0's and 1's.

The simulation results shown in Figure 8 confirm the functional shape of the result given in (13). The curves have a positive slope with respect to both ρ^2 (left to right along each curve) and η (bottom to top along any fixed vertical line), as required. The simulation VoM results track very closely with the prediction of the theory. For very small values of η, the theoretical curve provides a weaker upper bound. For larger values of η the upper bound is tighter.

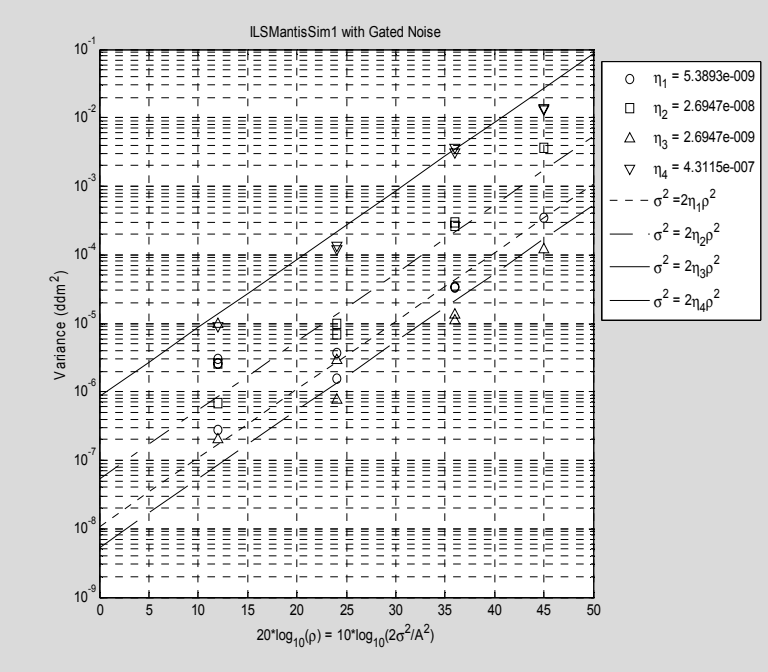

Figure 8 RFID Interference simulation results as a function of ρ^2

It is useful to compare the simulation results to the receiver instrumentation limits for GS and LOC established by [3] and [9], respectively. The comparison is shown in Figure 9. As expected, lower duty cycles (i.e., smaller values of η) permit larger interference power while maintaining the "shall-not-exceed" values. An average CIR over any single pulse of 0 dB can be supported by either system, even at fairly large values of η.

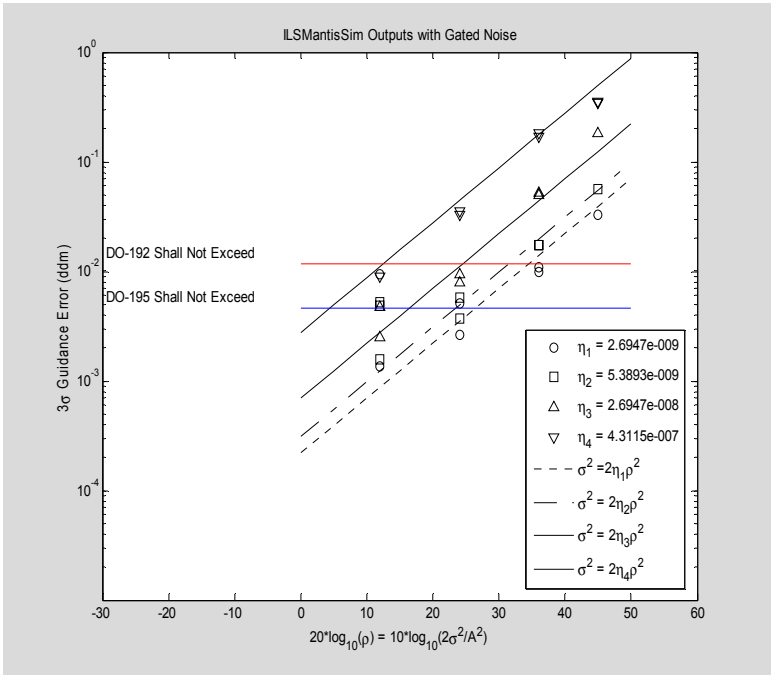

Figure 9 Comparison of simulation and theory with DO-192 and DO-195 limits

4.4 Consideration of Multiple Equipment Factor

One of the thorniest questions encountered during the work of SC-202 was the discussion of effects on sensitive avionics receivers of multiple RFID devices operating simultaneously on same aircraft. According to the procedures developed in [4], the effect of multiple devices is captured in a "multiple equipment factor" or MEF. For RFID devices operating with characteristics similar to the Mantis RFID tags considered in this report, it appears that the MEF is adequately accounted for by proper selection of the duty cycle, η.

If we make the reasonable assumption that an ensemble of RFID devices on a single aircraft are not synchronized, we can treat the transmission times as independent. The effective duty factor of each tag is then

$$\eta' = \eta \frac{B_{SA}}{B_{ILS}} = \frac{N_p t_p p_1}{T_{burst}} \approx 6 \times 10^{-4} \tag{19}$$

Therefore, the probability that two tags transmit at exactly the same time is small. Furthermore, because of the low cost of the RF tags the probability that two tags that *do* transmit at the same time remain synchronous is small. Therefore, we can assume that the effect of multiple RFID tags exhibits itself as an *increase* in the effective duty cycle of a hypothetical single composite tag. The effect of an increase in the effective duty cycle is already accounted for in (13). Therefore, the MEF effect for low duty-factor RFID tags, such as the Mantis tags considered in this study, can be included by artificially increasing the effective duty cycle.

4.5 Extrapolation to other Narrowband Systems

LOC and GS use exactly the same detection and demodulation process to obtain guidance signals. The output bandwidths specified by the relevant MOPS are identical. Therefore, the analysis for GS applies equally well to LOC, as well. As indicated in Figure 9, the LOC instrumentation error limits are much tighter. Fortunately, the measured emissions reported in [1] are significantly lower in the LOC band. Therefore the value of ρ^2 will also be lower in the LOC band, and the effects, in accordance with (13), will be correspondingly reduced.

The VHF Omnirange (VOR) system is guidance system operating in the VHF navigation band (108-118 MHz). VOR provides bearing information relative to known ground stations. The guidance bandwidth and signal processing is very similar to that of the LOC and GS functions. An analysis similar to that performed for ILS gives the fundamental variance relationship for VOR as

$$\sigma_{VOR}^2 = \frac{1}{m^2 CNR} \tag{20}$$

where m is the relevant index of modulation ($m = 0.3$), and σ_{VOR} is the standard deviation of the bearing guidance error in radians (*not* degrees!). Because the detection mechanism, the form of the VOR error equation and the VOR output bandwidth are comparable to those of LOC and GS, the impact of low-duty cycle RFID tag interference should be comparable, and should follow a form similar to (13). Confirmation of this conjecture was beyond the scope of the current task.

The key other VHF systems are VHF analog voice, VHF Data Link (VDL), and VHF Data Broadcast (VDB). Both systems have significantly larger bandwidth than the LOC, GS, and VOR systems and, therefore, will have different reactions in the presence of low-duty cycle RFID interference. Explicit study of these systems was beyond the scope of this report. In general,

however, we would expect that the very low level of emissions reported in [1] in the 108-136 MHz band – less than -70 dBm/100 kHz in all cases– and the low duty factors necessary to preserve RFID tag battery life, will result in no detectable effect on these systems. This expectation is supported by the link budget analyses in the follow section.

5 LINK BUDGET ANALYSES

In this section, we apply the process and simplified *pro forma* link budgets from DO-294B to six narrowband systems: GS, LOC, VOR, VDL Mode 2, Mode 3, VDB, and DSB-AM voice. When properly interpreted, the simplified link budget analyses indicate that the Mantis tags studied in this report should not pose an interference issue. If we can make the assumption that other RFID tag technology has similar effective duty cycles, these simple standardized analyses indicate that *most* situations should pose no interference problem. Only a small number of the cases indicate that further investigation is required, and these cases are not operationally relevant.

The *pro forma* analyses called out in DO-294B rely on the effective average emissions power of the T-PED device. From (13), we recognize that the effective duty cycle η, can be directly applied to the interference power, I, for as a starting point. For the methodology of DO-294B, it is appropriate to normalize the interference power to a 1 Hz bandwidth, as opposed to the 0.92 Hz bandwidth used in the analysis and simulations reported here. Therefore, we use a modified version of η:

$$\eta'' = \frac{\eta}{B_{ILS}} \tag{21}$$

5.1 GS

Table 1 provides the DO-294B *pro forma* analysis. The victim system is the ILS GS function. The source is the Mantis RFID tag with the following near-worst-case nominal parameters

$$\begin{aligned} t_p &= 10\ \mu\text{sec} \\ T_p &= 1.6\ \text{msec} \\ N_p &= 70 \\ p_0 &= p_1 = 0.5 \\ T_{burst} &= 0.6\ \text{sec} \\ B_{SA} &= 100\ \text{kHz} \\ B_{ILS} &= 0.92\ \text{Hz} \end{aligned} \tag{22}$$

from which we compute $\eta'' = -82.3$ dB/Hz. In particular, the value of $T_{BURST} = 0.6$ is very conservative.

Because the intentional emissions of the Mantis tags are close to the GS operating frequency, in this particular case the "intentionally radiated, antenna" (IRA) path loss (items 2 and 8) and the "non-intentionally radiate, antenna" (NIRA) path loss (item 18) are equal. The value of 50 dB has been chosen from the basic information in Appendix 5 of DO-294B for large cargo transportation aircraft (e.g., DC-10). It is important to note that the interference path loss (IPL) data collected in DO-294B is, in general, measured in the *cabin* and not the *cargo* hold of the aircraft, therefore, this value is only an estimate.

Under this assumption of 50 dB IPL, it is clear that the desensitization and spurious response show large margins, as indicated in lines 6 and line 12. The Mantis tags under consideration are, to the best available knowledge, not channelized but are time-orthogonal, therefore relevant low order intermodulation products in either the transmitter or receiver amplifier chains are not a problem (line 13). The low maximum transmit level (+5 dBm) and the IPL mean that the signal at the receiver input is unlikely to cause cross modulation effects (line 13A). The measured data reported in [1] does not reflect the presence of continuous wave tones, therefore the NIRA CW analysis of lines 14-20 is not applicable to this report.

Finally, the NIRA broadband interference analysis uses the maximum single-source Mantis tag emissions in the GS band reported by [1] (-30 dBm), reduced by the value of η'' computed from the values given in (22). The net effective *single entry* value for the NIRA power spectral density (PSD) is -112.3 dBm (line 26). The multiple equipment factor of 10 dB (line 24) is an assumption that is 3 dB more optimistic than the data reported in [1]. The rationale behind this more optimistic assumption is that only 10 Mantis tags will be located at positions that have the minimum IPL (50 dB) assumed in item 18.

Based on these two significant assumptions (50 dB path loss and 10 dB MEF) – both of which need to be verified – the Mantis tags should not pose a significant issue to ILS GS operations, despite their reported high emissions levels and relative proximity to the GS frequency band.

5.2 Localizer

Because the modulation is the same, the Localizer analysis exactly parallels that just described for GS. The results of the DO-294B *pro forma* analysis are shown in Table 2. The modifications for the LOC analysis include the following:

1. The IRA path loss is modified from the minimum path loss reported in DO-294B, Table 5-4 for LOC to account for additional loss at the 300 MHz Mantis operating frequency compared to the 100 MHz LOC operating frequency. A correction factor of 10 dB is used, roughly corresponding to $20\log_{10}(300\text{ MHz}/100\text{ MHz})$, which would be the correction for free space propagation. Although this is an assumption, the resulting margins are sufficient to accommodate any reasonable variation in the value encountered in real installations.

2. The NIRA path loss (item 18) is the *minimum* reported in DO-294B, Table 5-4.

3. The various susceptibility levels (items 1, 7, 17, and 23) have be modified to correspond to the values approved for DO-294B , Table 6-2.

4. The power spectral density (item 26) has been based on the maximum measured PSD for the Mantis tags in "Band 1", as reported by [1].

As with the GS analysis, the NIRA CW interference analysis in lines 14 through 22 is not particularly relevant given the measured data reported by [1]. The Analytical PSD margin (line 26) is sufficiently large to tolerate any of the Band 1 measured RFID emissions reported in [1] over a wide range of effective duty factors.

Table 1 DO-294B *pro forma* for Mantis tag interference to ILS GS at Cat I Decision Height

Simplified Link Budget for Susceptibility Analysis

Based on Table 6-3 from DO-294

Aircraft: Generic "Large Transport"

T-PED technology: Mantis RFID Tag, eta_prime = 5.8e-4

Receiver System: ILS Glide Slope at Cat I Decision Height

Desensitization (IRA)

Line	Item	Value	Units	Comments/Sources
1	Receiver out of band susceptibility	-16	dBm	From DO-294, Table 6-2.
2	IPL in T-PED Transmit Band (IRA IPL)	50	dB	Assumption based on large cargo aircraft. Because of close intentional frequency of Mantis tags, IRA IPL = NIRA IPL
3	Noise/desensitization MEF	0	dB	Low duty factor implies low probability of simultaneous emissions from multiple tags
4	Computed allowable emissions for T-PED	34	dBm	Use DO-294 Equation 6-1, using line items 1, 2 and 3, with differential gain term set to 0 dB.
5	Standards-based maximum EIRP on-channel emissions for single T-PED	5	dBm	Mantis Tag specification
6	**Desensitization margin**	**29**	**dB**	Computation

Spurious Response (IRA)

Line	Item	Value	Units	Comments/Sources
7	Receiver out of band spurious response	-16	dBm	From DO-294, Table 6-2.
8	IRA IPL	50	dB	Same as Line 2.
9	Noise/desensitization MEF	0	dB	Same as Line 3.
10	Computed allowable emissions for T-PED	34	dBm	Use DO-294 Equation 6-1, using line items 7, 8 and 9, with differential gain term set to 0 dB.
11	Standards-based maximum EIRP on-channel emissions for single T-PED	5	dBm	Mantis Tag specification
12	**Spurious response margin**	**29**	**dB**	Computation

Intermodulation (IRA - recvr generated, NIRA - tx. Generated)

Line	Item	Value	Units	Comments/Sources
13	Adjust standard analysis to aircraft-specific IPL and record minimum margin	99	dB	Low intentional power levels, close spacing to GS, indicate low IM power.

Cross Modulation (IRA)

Line	Item	Value	Units	Comments/Sources
13A	Compare measured IRA IPL to Table 6-4. "OK" if IRA IPL > appropriate value in Table 6-4.	OK		Line 2 value is 50 dB. Maximum GS entry in Table 6-4 < 50 dB, therefore cross modulation to GS should not be an issue

T-PED Undesired Emissions (NIRA narrowband and wideband)

Line	Item	Value	Units	Comments/Sources
14	Assumed net antenna gain (G_{AA})	-8	dBi	From DO-294, Table 6-2.
15	Measured aircraft net antenna gain (G_{AM})	-8	dBi	Assumption for this analysis
16	Analytical gain adjustment	0	dB	Computation
17	Aggregate CW interference level	-136.0	dBm	From DO-294, Table 6-2.
18	NIRA IPL	50	dB	Assumption based on large cargo aircraft.
19	CW MEF	0	dB	Single CW spur in GS bandwidth
20	Effective allowable emissions for single T-PED	-86.0	dBm	Computation
21	Standards-based CW emissions for single T-PED	-99	dBm	CW spur not considered in this analysis. NASA measurements do not indicate CW spur.
22	**Analytical CW margin**	**13**	**dB**	Computation
23	Aggregate PSD interference level	-142	dBm/Hz	From DO-294, Table 6-1.
24	Noise MEF	10	dB	MEF applied as linear in power per analysis
25	Computed allowable emissions for single T-PED	-102	dBm/Hz	Computation: Line 23+line 35-line24
26	Standards-based PSD emissions for single T-PED	-112.3	dBm/Hz	-30 dBm - 10log10(eta/0.92 Hz). -30 dBm value from single-entry measurement in NASA report at 334 MHz
27	**Analytical PSD margin**	**10.3**	**dB**	Computation

Bottom Line

28	**IRA OK for this source-victim combination?**	**YES**	YES/ NEXT STEP	"YES" if lines 6, 12, and 13 are all > 10 dB, and 13A is "OK". Otherwise, "Next Step".
29	**NIRA OK for this source-victim combination?**	**YES**	YES/ NEXT STEP	"YES" if lines 22 and 27 both >10 dB. Otherwise "NEXT STEP"

Table 2 DO-294B *pro forma* for Mantis tag interference to ILS LOC at Cat I Decision Height

Simplified Link Budget for Susceptibility Analysis

Based on Table 6-3 from DO-294

Aircraft: Generic "Large Transport"
T-PED technology: Mantis RFID Tag, eta_prime = 5.8e-4
Receiver System: Localizer at Cat I DH

Desensitization (IRA)

Line	Item	Value	Units	Comments/Sources
1	Receiver out of band susceptibility	-26	dBm	From DO-294, Table 6-2.
2	IPL in T-PED Transmit Band (IRA IPL)	45	dB	NIRA IPL extrapolated for frequency
3	Noise/desensitization MEF	0	dB	Low duty factor implies low probability of simultaneous emissions from multiple tags
4	Computed allowable emissions for T-PED	19	dBm	Use DO-294 Equation 6-1, using line items 1, 2 and 3, with differential gain term set to 0 dB.
5	Standards-based maximum EIRP on-channel emissions for single T-PED	5	dBm	Mantis Tag specification
6	**Desensitization margin**	**14**	**dB**	Computation

Spurious Response (IRA)

Line	Item	Value	Units	Comments/Sources
7	Receiver out of band spurious response	-26	dBm	From DO-294, Table 6-2.
8	IRA IPL	45	dB	Same as Line 2.
9	Noise/desensitization MEF	0	dB	Same as Line 3.
10	Computed allowable emissions for T-PED	19	dBm	Use DO-294 Equation 6-1, using line items 7, 8 and 9, with differential gain term set to 0 dB.
11	Standards-based maximum EIRP on-channel emissions for single T-PED	5	dBm	Mantis Tag specification
12	**Spurious response margin**	**14**	**dB**	Computation

Intermodulation (IRA - recvr generated, NIRA - tx. Generated)

Line	Item	Value	Units	Comments/Sources
13	Adjust standard analysis to aircraft-specific IPL and record minimum margin	none	dB	Low intentional power levels, high IM immunity of LOC receiver indicate no IM issues.

Cross Modulation (IRA)

Line	Item	Value	Units	Comments/Sources
13A	Compare measured IRA IPL to Table 6-4. "OK" if IRA IPL > appropriate value in Table 6-4.	OK		Line 2 value is 45 dB. Maximum Localizer entry in Table 6-4 < 45 dB, therefore cross modulation to Localizer should not be an issue

T-PED Undesired Emissions (NIRA narrowband and wideband)

Line	Item	Value	Units	Comments/Sources
14	Assumed net antenna gain (G_{AA})	-7	dBi	From DO-294, Table 6-2.
15	Measured aircraft net antenna gain (G_{AM})	-7	dBi	Assumption for this analysis
16	Analytical gain adjustment	0	dB	Computation
17	Aggregate CW interference level	-144.5	dBm	From DO-294, Table 6-2.
18	NIRA IPL	35	dB	Assumption based on large cargo aircraft.
19	CW MEF	0	dB	Single CW spur in LOC bandwidth
20	Effective allowable emissions for single T-PED	-109.5	dBm	Computation
21	Standards-based CW emissions for single T-PED	-130	dBm	CW spur not considered in this analysis. NASA measurements do not indicate CW spur.
22	**Analytical CW margin**	**20.5**	**dB**	Computation
23	Aggregate PSD interference level	-151	dBm/Hz	From DO-294, Table 6-2.
24	Noise MEF	10	dB	MEF applied as linear in power per analysis
25	Computed allowable emissions for single T-PED	-126	dBm/Hz	Computation: Line 23+line 35-line24
26	Standards-based PSD emissions for single T-PED	-182.3	dBm/Hz	-100 dBm - 10log10(eta/0.92 Hz), per NASA report, Figure 3.3-1
27	**Analytical PSD margin**	**56.3**	**dB**	Computation

28	**IRA OK for this source-victim combination?**	**YES**	YES/ NEXT STEP	"YES" if lines 6, 12, and 13 are all >= 10 dB, and 13A is "OK". Otherwise, "Next Step".
29	**NIRA OK for this source-victim combination?**	**YES**	YES/ NEXT STEP	"YES" if lines 22 and 27 both >=10 dB. Otherwise "NEXT STEP"

5.3 VOR

The VOR analysis is very similar to that of LOC. The results of the DO-294B *pro forma* analysis are shown in Table 3. The modifications for the VOR analysis include the following:

1. The IRA path loss is modified in the same manner used for the LOC analysis to account for the difference between the VOR and Mantis tag operating frequencies.

2. The NIRA path loss (item 18) is the *minimum* reported in DO-294B, Table 5-4.

3. The various susceptibility levels (items 1, 7, 17, and 23) have be modified to correspond to the values approved for DO-294B , Table 6-2.

4. The power spectral density (item 26) has been based on the maximum measured PSD for the Mantis tags in "Band 1", as reported by [1].

Once again, the NIRA CW analysis in lines 14-22 is not particularly relevant, given the measured emissions spectra report in [1]. The Analytical PSD margin (line 26) is sufficiently large to tolerate any of the Band 1 measured RFID emissions reported in [1] over a 13 dB range of effective duty factors (or, equivalently, MEF values), without requiring on-aircraft testing. This result is *conservative*, in the sense that it uses the *minimum* IPL measured in the aircraft *cabin*, as reported in DO-294B, Table 5-4.

5.4 DSB-AM Voice

We now consider the equivalent *pro forma* analysis for the classic conventional double-sideband amplitude modulated (DSB-AM) analog voice communications in the VHF band from 118-136 MHz. This analysis is not intended to be the final word on the immunity of DSB-AM voice systems to the on-board use of RFID tags, but rather to take a "first look" at the issue and ascertain if additional study and analysis are required.

Previous studies regarding interference levels with DSB-AM voice as the victim system and VHF Data Link (VDL) Mode 2, Mode 3 and Mode 4 as the source have indicated that DSB-AM is annoyingly susceptible to pulsed interference with relatively low duty cycle. This interference exhibits itself as a series of clicks in the audio output of the DSB-AM receiver that are distracting to the pilot users. Based on this previous experience, then, we will assume that it is *inappropriate* to take advantage of the effective duty cycle, η, and will concentrate this analysis based on the power in a single RFID pulse, as measured by the peak measurement methodology of [1].

The results of the DO-294B *pro forma* analysis are shown in Table 3. The modifications for the VOR analysis include the following:

1. The IRA path loss is modified in the same manner used for the LOC analysis to account for the difference between the DSB-AM and Mantis tag operating frequencies.

2. The NIRA path loss (item 18) is the *minimum* reported in DO-294B, Table 5-4.

Table 3 DO-294B *pro forma* for Mantis tag interference to VOR

Simplified Link Budget for Susceptibility Analysis

Based on Table 6-4 from DO-294

Aircraft: Generic "Large Transport"
T-PED technology: Mantis RFID Tag, eta_prime = 5.8e-4
Receiver System: VOR

Desensitization (IRA)

Line	Item	Value	Units	Comments/Sources
1	Receiver out of band susceptibility	-13	dBm	From DO-294, Table 6-2.
2	IPL in T-PED Transmit Band (IRA IPL)	40	dB	Adjusted for frequency
3	Noise/desensitization MEF	0	dB	Low duty factor implies low probability of simultaneous emissions from multiple tags
4	Computed allowable emissions for T-PED	27	dBm	Use DO-294 Equation 6-1, using line items 1, 2 and 3, with differential gain term set to 0 dB.
5	Standards-based maximum EIRP on-channel emissions for single T-PED	5	dBm	Mantis Tag specification
6	**Desensitization margin**	**22**	**dB**	Computation

Spurious Response (IRA)

Line	Item	Value	Units	Comments/Sources
7	Receiver out of band spurious response	-13	dBm	From DO-294, Table 6-2.
8	IRA IPL	40	dB	Same as Line 2.
9	Noise/desensitization MEF	0	dB	Same as Line 3.
10	Computed allowable emissions for T-PED	27	dBm	Use DO-294 Equation 6-1, using line items 7, 8 and 9, with differential gain term set to 0 dB.
11	Standards-based maximum EIRP on-channel emissions for single T-PED	5	dBm	Mantis Tag specification
12	**Spurious response margin**	**22**	**dB**	Computation

Intermodulation (IRA - recvr generated, NIRA - tx. Generated)

Line	Item	Value	Units	Comments/Sources
13	Adjust standard analysis to aircraft-specific IPL and record minimum margin	99	dB	Low intentional power levels, high IM immunity of VOR receiver indicate no IM issues.

Cross Modulation (IRA)

Line	Item	Value	Units	Comments/Sources
13A	Compare measured IRA IPL to Table 6-4. "OK" if IRA IPL > appropriate value in Table 6-4.	OK		Line 2 value is 30 dB. Maximum Localizer entry in Table 6-4 < 30 dB, therefore cross modulation to Localizer should not be an issue

T-PED Undesired Emissions (NIRA narrowband and wideband)

Line	Item	Value	Units	Comments/Sources
14	Assumed net antenna gain (G_{AA})	-7	dBi	From DO-294, Table 6-2.
15	Measured aircraft net antenna gain (G_{AM})	-7	dBi	Assumption for this analysis
16	Analytical gain adjustment	0	dB	Computation
17	Aggregate CW interference level	-145	dBm	From DO-294, Table 6-2.
18	NIRA IPL	30	dB	Assumption based on large cargo aircraft.
19	CW MEF	0	dB	Single CW spur in LOC bandwidth
20	Effective allowable emissions for single T-PED	-115.0	dBm	Computation
21	Standards-based CW emissions for single T-PED	-130	dBm	CW spur not considered in this analysis. NASA measurements do not indicate CW spur.
22	**Analytical CW margin**	**15.0**	**dB**	Computation
23	Aggregate PSD interference level	-147	dBm/Hz	From DO-294, Table 6-2.
24	Noise MEF	10	dB	MEF applied as linear in power per analysis
25	Computed allowable emissions for single T-PED	-127	dBm/Hz	Computation: Line 23+line 35-line24
26	Standards-based PSD emissions for single T-PED	-150	dBm/Hz	-100 dBm - 10log10(100 kHz), per NASA report, Figure 3.3-1. This is the computation for eta_prime = 1, and gives the worst case single-symbol CNR
27	**Analytical PSD margin**	**23.0**	**dB**	Computation still shows large margin

28	**IRA OK for this source-victim combination?**	**YES**	YES/ NEXT STEP	"YES" if lines 6, 12, and 13 are all >= 10 dB, and 13A is "OK". Otherwise, "Next Step".
29	**NIRA OK for this source-victim combination?**	**YES**	YES/ NEXT STEP	"YES" if lines 22 and 27 both >=10 dB. Otherwise "NEXT STEP"

Table 4 DO-294B *pro forma* for Mantis tag interference to DSB-AM VHF Analog Voice

Simplified Link Budget for Susceptibility Analysis

Based on Table 6-4 from DO-294

Aircraft: Generic "Large Transport"
T-PED technology: Mantis RFID Tag, eta_prime = 5.8e-4
Receiver System: VHF DSB-AM Voice

Desensitization (IRA)

Line	Item	Value	Units	Comments/Sources
1	Receiver out of band susceptibility	-7	dBm	From DO-294, Table 6-2.
2	IPL in T-PED Transmit Band (IRA IPL)	35	dB	Adjusted for frequency
3	Noise/desensitization MEF	0	dB	Low duty factor implies low probability of simultaneous emissions from multiple tags
4	Computed allowable emissions for T-PED	28	dBm	Use DO-294 Equation 6-1, using line items 1, 2 and 3, with differential gain term set to 0 dB.
5	Standards-based maximum EIRP on-channel emissions for single T-PED	5	dBm	Mantis Tag specification
6	**Desensitization margin**	**23**	**dB**	Computation

Spurious Response (IRA)

Line	Item	Value	Units	Comments/Sources
7	Receiver out of band spurious response	-33	dBm	From DO-294, Table 6-2.
8	IRA IPL	35	dB	Same as Line 2.
9	Noise/desensitization MEF	0	dB	Same as Line 3.
10	Computed allowable emissions for T-PED	2	dBm	Use DO-294 Equation 6-1, using line items 7, 8 and 9, with differential gain term set to 0 dB.
11	Standards-based maximum EIRP on-channel emissions for single T-PED	5	dBm	Mantis Tag specification
12	**Spurious response margin**	**-3**	**dB**	Computation

Intermodulation (IRA - recvr generated, NIRA - tx. Generated)

Line	Item	Value	Units	Comments/Sources
13	Adjust standard analysis to aircraft-specific IPL and record minimum margin	99	dB	Low intentional power levels, high IM immunity of VOR receiver indicate no IM issues.

Cross Modulation (IRA)

Line	Item	Value	Units	Comments/Sources
13A	Compare measured IRA IPL to Table 6-4. "OK" if IRA IPL > appropriate value in Table 6-4.	OK		Line 2 value is 40 dB. Maximum Localizer entry in Table 6-4 < 40 dB, therefore cross modulation to DSB-AM should not be an issue

T-PED Undesired Emissions (NIRA narrowband and wideband)

Line	Item	Value	Units	Comments/Sources
14	Assumed net antenna gain (G_{AA})	-7	dBi	From DO-294, Table 6-2.
15	Measured aircraft net antenna gain (G_{AM})	-7	dBi	Assumption for this analysis
16	Analytical gain adjustment	0	dB	Computation
17	Aggregate CW interference level	-142.5	dBm	From DO-294, Table 6-2.
18	NIRA IPL	25	dB	Assumption based on large cargo aircraft.
19	CW MEF	0	dB	Single CW spur in LOC bandwidth
20	Effective allowable emissions for single T-PED	-117.5	dBm	Computation
21	Standards-based CW emissions for single T-PED	-130	dBm	CW spur not considered in this analysis. NASA measurements do not indicate CW spur.
22	**Analytical CW margin**	**12.5**	**dB**	Computation
23	Aggregate PSD interference level	-152	dBm/Hz	From DO-294, Table 6-2.
24	Noise MEF	10	dB	MEF applied as linear in power per analysis
25	Computed allowable emissions for single T-PED	-137	dBm/Hz	Computation: Line 23+line 35-line24
26	Standards-based PSD emissions for single T-PED	-150	dBm/Hz	-100 dBm - 10log10(100 kHz), per NASA report, Figure 3.3-1. This is the computation for eta_prime = 1, and gives the worst case CNR, i.e., the CNR within a "click"
27	**Analytical PSD margin**	**13.0**	**dB**	Computation still shows large margin

28	**IRA OK for this source-victim combination?**	**NEXT STEP**	YES/ NEXT STEP	"YES" if lines 6, 12, and 13 are all >= 10 dB, and 13A is "OK". Otherwise, "Next Step".
29	**NIRA OK for this source-victim combination?**	**YES**	YES/ NEXT STEP	"YES" if lines 22 and 27 both >=10 dB. Otherwise "NEXT STEP"

3. The various susceptibility levels (items 1, 7, 17, and 23) have be modified to correspond to the values approved for DO-294B , Table 6-2.

4. The power spectral density (item 26) has been based on the maximum measured PSD for the Mantis tags in "Band 1", as reported by [1], adjusted only by the measurement bandwidth of 100 kHz to get a power spectral density result.

5. The NIRA MEF is set to 0 dB. This assumption is tied to our intent of representing the *individual pulse* effect on DSB-AM. It reflects the fact that given the low effective pulse duty cycle of RFID tag devices, there is a corresponding low probability that two pulses from different tags will be transmitted at the same time. Therefore, when considering the individual pulse effects on DSB-AM, we need only consider these individual pulses one pulse at a time.[11]

As with GS, LOC, and VOR, the results indicate that desensitization, intermodulation, cross modulation, and NIRA noise-like interference should not be an issue. This is a very positive result, as these computations are *not* based on the low RFID duty factor, as noted above. As with GS, LOC, and VOR, the section on NIRA CW interference is not particularly relevant due to the lack of CW emissions characteristics reported by [1].

Unlike the GS, LOC, and VOR analyses, however, item 12 indicates a potential issue with spurious response of the DSB-AM receiver. The computed margin (item 12) is -3 dB, indicating that on-aircraft measurement is required. In this particular case, the DO-294B *pro forma* methodology is probably *overly conservative*. The spurious response specification in DO-186 is intended to provide relief for low-cost DSB-AM receivers that may lack appropriate image rejection. In general, receiver designers take particular care in rejection of the odd harmonics of the local oscillator and desired signals. Therefore, although this matter bears additional investigation, it may not be an issue in practical DSB-AM receiver designs.

5.5 VDL Mode 2/3 and VDB

Like DSB-AM analog voice, the VDL Mode 2, Mode 3 and VHF Data Broadcast (VDB) waveforms are more susceptible to pulsed interference. VDL Mode 2, Mode 3, and VDB use a differential eight-phase modulation (D8PSK) at a rate of 10,500 symbols per second. The information is encoded via a Reed-Solomon code for forward error correction. The Reed-Solomon code has specific strengths in the correction of bursty error patterns, such as those that might occur due to a single Mantis RFID tag. Therefore, this analysis will once again focus on single pulse errors. As in the DSB-AM case, this analysis is not intended to be the final word on the immunity of D8PSK data systems to the on-board use of RFID tags, but rather to take a "first look" at the issue and ascertain if additional study and analysis are required.

The VDL Mode 2, Mode 3, and VDB analysis is very similar to that for DSB-AM. The results of the DO-294B *pro forma* analysis are shown in Table 5. The modifications for the VDL analysis include the following:

1. The IRA path loss is modified in the same manner used for the LOC analysis to account for the difference between the VDL Mode 2, Mode 3 and VDB operating frequencies and the Mantis tag operating frequencies.

2. The NIRA path loss (item 18) is the *minimum* reported in DO-294B, Table 5-4.

[11] Assuming that overlapping pulses commonly occur would be equivalent to assuming that the RFID tag readers could distinguish overlapping IDs.

3. The various susceptibility levels (items 1, 7, 17, and 23) have be modified to correspond to the values approved for DO-294B , Table 6-2.

4. The power spectral density (item 26) has been based on the maximum measured PSD for the Mantis tags in "Band 1", as reported by [1], adjusted only by the measurement bandwidth of 100 kHz to get a power spectral density result.

5. The NIRA MEF is set to 0 dB. This assumption is tied to our intent of representing the *individual pulse* effect on D8PSK. It reflects the fact that given the low effective pulse duty cycle of RFID tag devices, there is a corresponding low probability that two pulses from different tags will be transmitted at the same time. Therefore, when considering the individual pulse effects on DSB-AM, we need only consider these individual pulses one pulse at a time.

In this case, two of the receiver parameters show analytical margins below the 10 dB threshold established by DO-294B. As with the DSB-AM results in the previous section the spurious response parameter indicates that additional testing is required. This conclusion may be overly conservative for the same reasons given for DSB-AM. The analytical PSD margin (line 27), is also below the 10 dB threshold. We note, however, that the margin remains significant at 6 dB above the conservative susceptibility threshold contained in DO-294. For these digital communication systems, the relevant receiver output parameter is the either the uncorrected bit error rate or the received word error rate. The effect of slightly decreased broadband CNR during the pulse duration is an increased channel bit error rate, but this effect is *exponentially decreasing* with the CNR. At the channel bit error rates of interest, the 6 dB margin shown in Table 5 is equivalent to a received word error rate significantly less than 10^{-4}.

Table 5 DO-294B *pro forma* for Mantis tag interference toVDL Mode 2/3 digital communications

Simplified Link Budget for Susceptibility Analysis

Based on Table 6-4 from DO-294

Aircraft: Generic "Large Transport"
T-PED technology: Mantis RFID Tag, eta_prime = 1
Receiver System: VDL Mode 2, Mode 3, VDB

Desensitization (IRA)

Line	Item	Value	Units	Comments/Sources
1	Receiver out of band susceptibility	-7	dBm	From DO-294, Table 6-2.
2	IPL in T-PED Transmit Band (IRA IPL)	35	dB	Adjusted for frequency
3	Noise/desensitization MEF	0	dB	Low duty factor implies low probability of simultaneous emissions from multiple tags
4	Computed allowable emissions for T-PED	28	dBm	Use DO-294 Equation 6-1, using line items 1, 2 and 3, with differential gain term set to 0 dB.
5	Standards-based maximum EIRP on-channel emissions for single T-PED	5	dBm	Mantis Tag specification
6	**Desensitization margin**	**23**	**dB**	Computation

Spurious Response (IRA)

Line	Item	Value	Units	Comments/Sources
7	Receiver out of band spurious response	-33	dBm	From DO-294, Table 6-2.
8	IRA IPL	35	dB	Adjusted for frequency
9	Noise/desensitization MEF	0	dB	Same as Line 3.
10	Computed allowable emissions for T-PED	2	dBm	Use DO-294 Equation 6-1, using line items 7, 8 and 9, with differential gain term set to 0 dB.
11	Standards-based maximum EIRP on-channel emissions for single T-PED	5	dBm	Mantis Tag specification
12	**Spurious response margin**	**-3**	**dB**	Computation, see discussion in text.

Intermodulation (IRA - recvr generated, NIRA - tx. Generated)

Line	Item	Value	Units	Comments/Sources
13	Adjust standard analysis to aircraft-specific IPL and record minimum margin	99	dB	Low intentional power levels, high IM immunity of VDL receiver indicate no IM issues.

Cross Modulation (IRA)

Line	Item	Value	Units	Comments/Sources
13A	Compare measured IRA IPL to Table 6-4. "OK" if IRA IPL > appropriate value in Table 6-4.	OK		Line 2 value is 25 dB. Maximum Localizer entry in Table 6-4 < 25 dB, therefore cross modulation to Localizer should not be an issue

T-PED Undesired Emissions (NIRA narrowband and wideband)

Line	Item	Value	Units	Comments/Sources
14	Assumed net antenna gain (G_{AA})	-7	dBi	From DO-294, Table 6-2.
15	Measured aircraft net antenna gain (G_{AM})	-7	dBi	Assumption for this analysis
16	Analytical gain adjustment	0	dB	Computation
17	Aggregate CW interference level	-131.0	dBm	From DO-294, Table 6-2.
18	NIRA IPL	25	dB	Assumption based on large cargo aircraft.
19	CW MEF	0	dB	Single CW spur in LOC bandwidth
20	Effective allowable emissions for single T-PED	-106.0	dBm	Computation
21	Standards-based CW emissions for single T-PED	-130	dBm	CW spur not considered in this analysis. NASA measurements do not indicate CW spur.
22	**Analytical CW margin**	**24.0**	**dB**	Computation
23	Aggregate PSD interference level	-159	dBm/Hz	From DO-294, Table 6-2.
24	Noise MEF	10	dB	MEF applied as linear in power per analysis
25	Computed allowable emissions for single T-PED	-144	dBm/Hz	Computation: Line 23+line 35-line24
26	Standards-based PSD emissions for single T-PED	-150	dBm/Hz	-100 dBm - 10log10(100,000), per NASA report, Figure 3.3-1
27	**Analytical PSD margin**	**6.0**	**dB**	Computation, see discussion in text.

28	**IRA OK for this source-victim combination?**	**NEXT STEP**	YES/ NEXT STEP	"YES" if lines 6, 12, and 13 are all >= 10 dB, and 13A is "OK". Otherwise, "Next Step".
29	**NIRA OK for this source-victim combination?**	**NEXT STEP**	YES/ NEXT STEP	"YES" if lines 22 and 27 both >=10 dB. Otherwise "NEXT STEP"

6 CONCLUSIONS

Based on the analysis in the previous sections, we can reach several conclusions regarding the effects of RFID tags in general, and specifically Mantis tags, on the narrowband VHF and UHF aeronautical radio systems.

1. The effect of low-duty cycle RFID tags on the guidance output of the narrowband navigation system (GS, LOC, VOR) is proportional to the effective duty cycle of the transmissions and inversely proportion to the carrier to interference ratio at the receiver input, as measured during the duration of a single pulse. This relation is expressed in equation (13).

2. Simulations of generic ILS receiver processing confirm the form of (13) for pulsed noise-like interference.

3. When the effective average interference levels predicted by (13) are used, the *pro forma* analysis recommended by Section 6 DO-294B indicates that the effects of RFID emissions ILS GS are probably negligible on large cargo aircraft.

4. When the effective average interference levels predicted by (13) are used, the *pro forma* analysis recommended by Section 6 of DO-294B indicates that the effects of RFID emissions ILS LOC and VOR receivers should be negligible across a wide range of aircraft, duty cycle, and multiple equipment factor considerations.

5. When single-pulse interference levels are considered, the effects of relatively low-power (5 dBm) RFID tags on DSB-AM and D8PSK VHF communications systems should be negligible. This conclusion is subject to the caveat that the spurious response susceptibility to intentional emission of RFID tags remains an open question that bears further examination by either analysis or measurement, or both.

7 RECOMMENDATIONS

1. The conclusion regarding GS is based on several assumptions regarding the operational use of the RFID tags – specifically Mantis tags – on aircraft. While these assumptions appear to be reasonable based on information reported in DO-294B, some additional investigation of the following parameters should be undertaken:

    a. Representative IPL measurements in the bands of both the intentional emissions of the RFID tag and the operational band of the victim receivers (e.g., LOC, VOR, GS, etc) should be taken for locations in the cargo bays of large commercial aircraft. Measurements on cargo aircraft, which are mostly missing from the DO-294B data, should be considered a priority.

    b. Based on the representative measurements, an analysis indicating the number of potential RFID tags with the minimum IRA/NIRA IPL should be performed.

2. The models used here consider a pulsed-noise form of interference from the RFID tags. These results should be extended to consider pulsed-CW forms of interference. Preliminary results conducted during the preparation of this report indicate that the allowable interference will be somewhat lower, but there remain open issues between the preliminary simulation and analysis results. This report has concentrated on the pulse-noise model, as that model appears to best describe the emissions spectra reported in [1].

3. Additional analysis of DSB-AM voice susceptibility to the pulsed interference from RFID tags should be considered. In particular, this analysis should focus on susceptibilities that could be classified as "spurious response", in accordance with the *pro forma* table established by Section 6 of DO-294B. Such analyses should specifically consider the pilot acceptance factors of spurious "clicking" in the DSB-AM output. Preliminary work performed for the VDL Mode 4 Integration study for Eurocontrol [13] may be applicable to this analysis.[12]

4. Additional analysis of D8PSK digital data susceptibility to the pulsed interference from RFID tags should be considered. In particular, this analysis should focus on susceptibilities that could be classified as "spurious response", in accordance with the *pro forma* table established by Section 6 of DO-294B. Such analyses should specifically consider the burst effects of the interference and the error-correcting capabilities of the Mode 2/3 signal format.

5. An analysis similar to that reported here should be considered for the remaining systems listed in Table 6-2 of DO-294B.

[12] Unfortunately, limitations on the current effort did not allow consideration of these effects in this report.

APPENDIX A. Acronyms and Abbreviations

AWGN	Additive White Gaussian Noise
CNR	Carrier power-to-Noise power ratio
CW	Continuous Wave
D8PSK	Differentially encoded 8 Phase Shift Keying
dBm	Decibels with respect to one milliwatt = $10\log_{10}$(Power/1 mw)
ddm	Difference in Depth of Modulation
DSB-AM	Double Sideband Amplitude Modulation
FCC	Federal Communications Commission
GS	Glide Slope
Hz	Hertz, 1 Hz = 1 cycle per second
IF	Intermediate Frequency
ILS	Instrument Landing System
IPL	Interference Path Loss
IRA	Intentionally Radiated-to-victim-Antenna (coupling path)
LOC	Localizer
MEF	Multiple Equipment Factor
MHz	Megahertz = 10^6 cycles per second
MoV	Mean of Variances
NASA	National Aeronautics and Space Administration
NIRA	Non-Intentionally Radiated-to-victim-Antenna (coupling path)
OOK	On-Off Keying
PAM	Pulse Amplitude Modulation
PSD	Power Spectral Density
RF	Radio Frequency
RFID	Radio Frequency Identification (tag)
T-PED	(Intentionally) Transmitting Portable Electronic Device
UHF	Ultra High Frequency
VDB	VHF Data Broadcast
VDL	VHF Data Link
VHF	Very High Frequency
VoM	Variance of Means
VOR	Very High Frequency Omnirange

.

APPENDIX B. Simulation Waveforms

This appendix contains waveforms from a typical simulation run. These waveforms were generated using a pulsed-CW model for the interference so that certain aspects of the simulation were more clearly shown, thereby validating the simulated processing. As noted in the main body of the report, the results reported in the main body of this report were obtained using a pulsed-noise model which more accurately describes the measurements reported in [1].

Simulation parameters: ILS on-course GS, Mantis 10 μsec pulses spaced 1.6 ms apart, random data PAM (OOK) with Pr{1}=Pr{0}=0.5, 70 pulse slots per burst, identical bursts repeat every 0.6 seconds. Mantis pulses modeled as pulsed CW. This roughly represents a single worst-case Mantis tag in high stress environment (maximum repetition rate)

Simulation access point	Time domain (all x-axes in seconds, y-axes in "volts")	Frequency Domain (all x-axes in Hz, y-axes in decibels relative to total unmodulated carrier power)
Perfect ILS GS	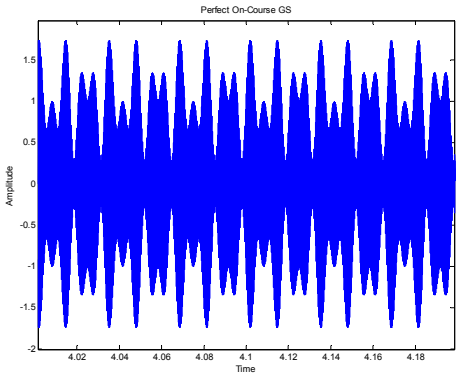	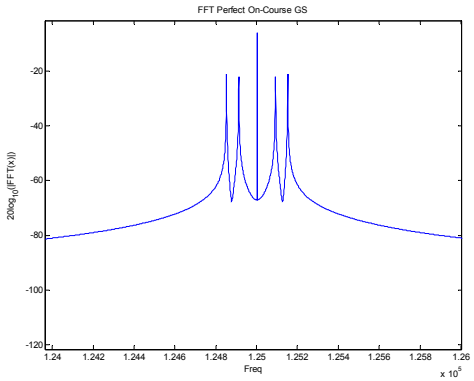
Idealized Mantis sub-burst w/ random data, unity amplitude, gated sinusoid	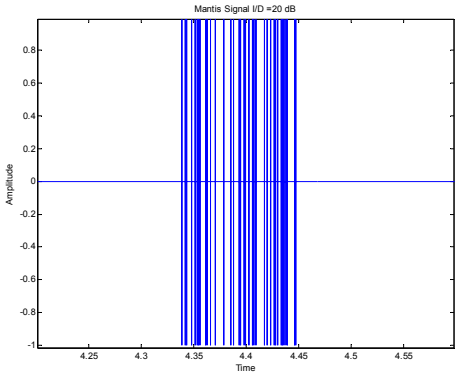	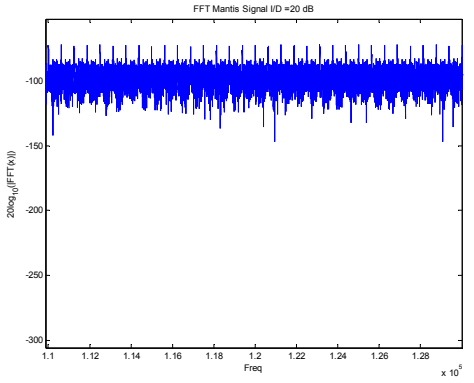

Simulation access point	Time domain (all x-axes in seconds, y-axes in "volts")	Frequency Domain (all x-axes in Hz, y-axes in decibels relative to total unmodulated carrier power)
Idealized composite signal, unity amplitude GS, rho = 10 (i.e. 20 dB)	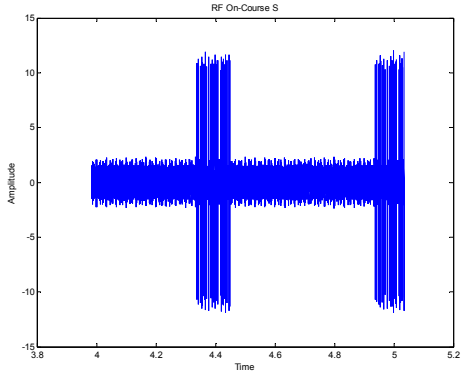	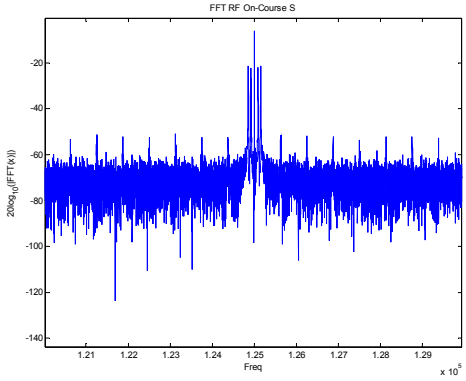
IF filter output, BW=40 kHz	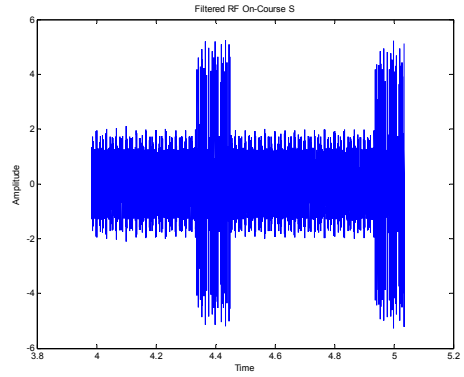	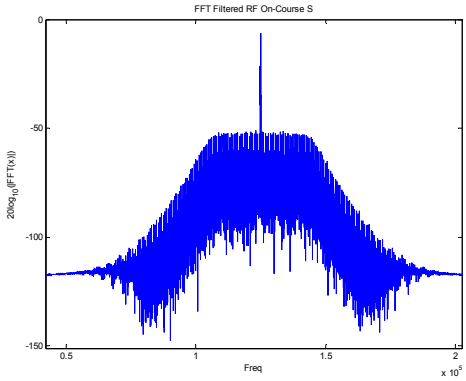
Detected envelope, with low-pass, anti-aliasing filter	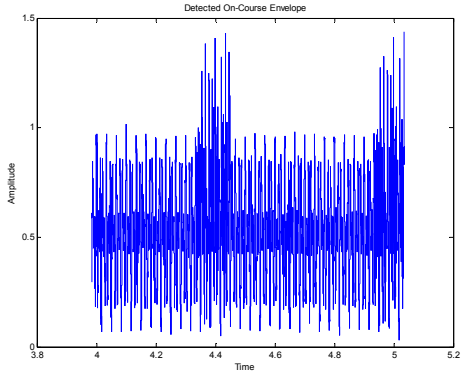	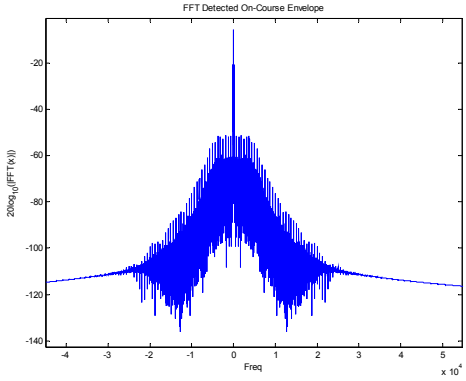

Simulation access point	Time domain (all x-axes in seconds, y-axes in "volts")	Frequency Domain (all x-axes in Hz, y-axes in decibels relative to total unmodulated carrier power)
Detected envelope, downsampled	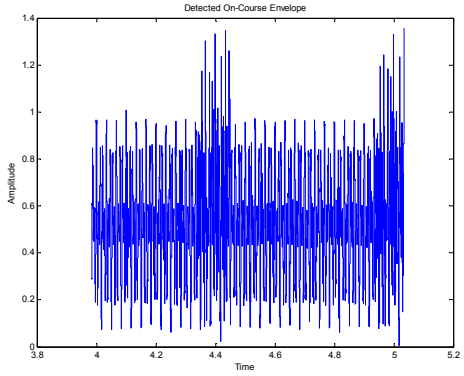	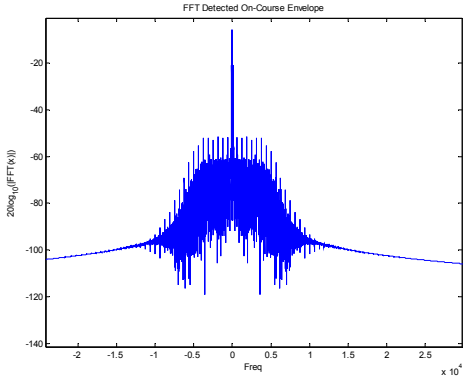
Output of 90 Hz BPF	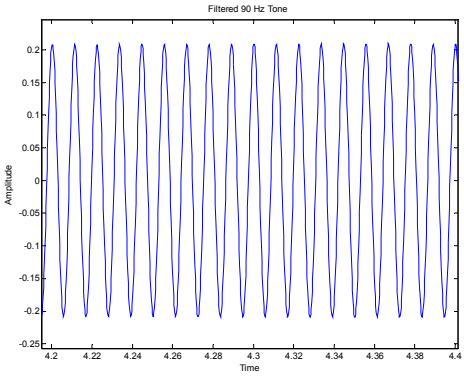	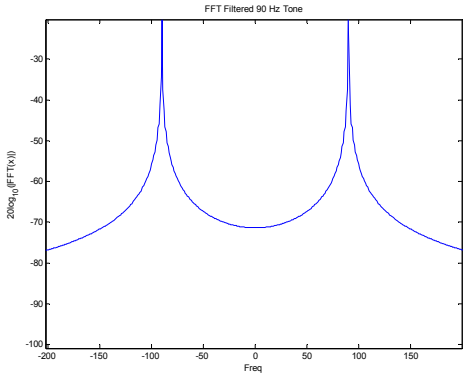
Output of 150 Hz BPF	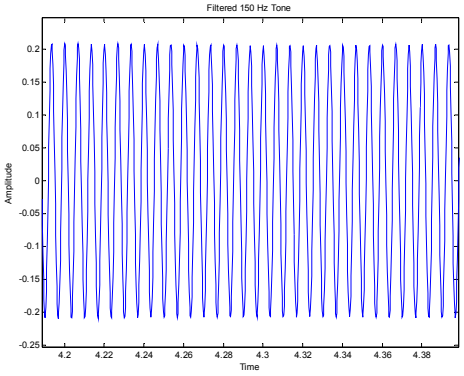	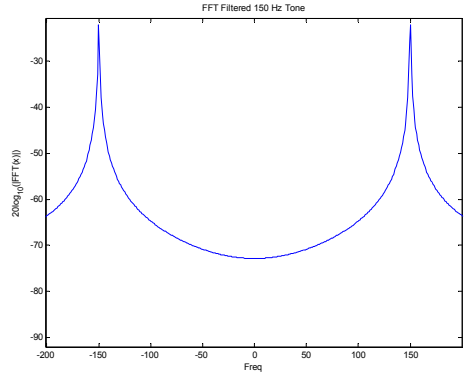

Simulation access point	Time domain (all x-axes in seconds, y-axes in "volts")	Frequency Domain (all x-axes in Hz, y-axes in decibels relative to total unmodulated carrier power)
Detected 90 Hz tone level (notice low level spurious responses)	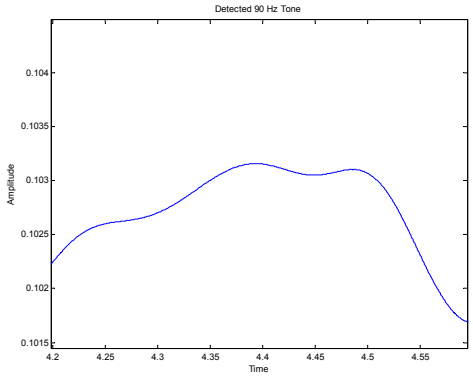	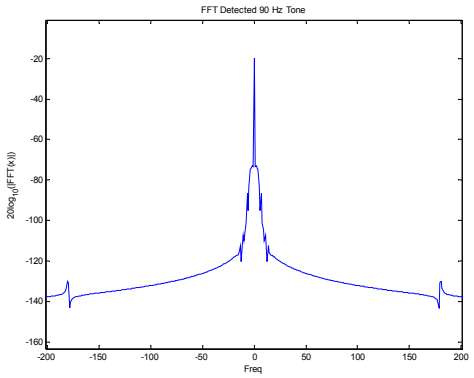
Detected 150 Hz tone level	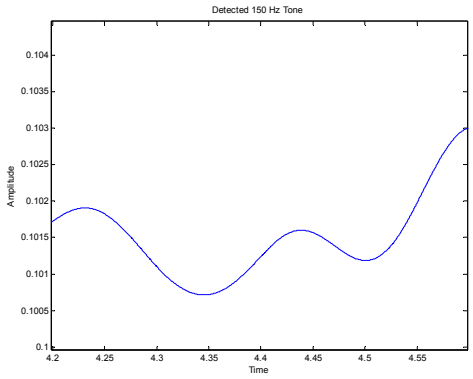	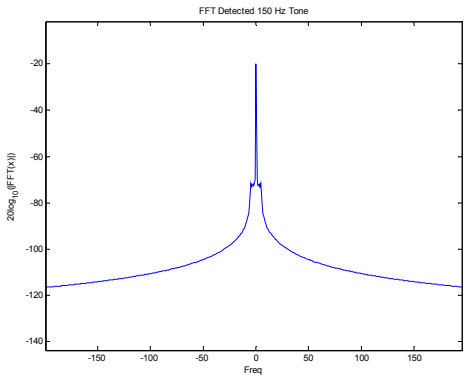
90 & 150 Hz, raw ddm, filtered ddm	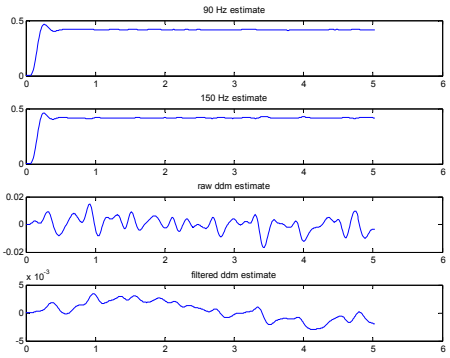	

References

[1] T. X. Nguyen, J. J. Ely, R. A. Williams, S. V. Koppen, and M. T. Salud, "RFID Transponders' Radio Frequency Emissions in Aircraft Communication and Navigation Radio Bands," NASA Langley Research Center, Hampton, VA, NASA/TP-2006-214295, March, 2006.

[2] "Annex 10 to the Convention on International Civil Aviation, Fifth Edition," ICAO, Montreal, I (Radio Naviation Aids), 1996.

[3] "Minimum Operational Performance Standards for Airborne ILS Glide Slope Receiving Equipment Within the Radio Frequency Range of 328.6-335.4 MHz," RTCA, Washington, D.C., DO-192, 1986.

[4] "Guidance on Allowing Transmitting Portable Electronic Devices (T-PEDs) on Aircraft," RTCA, Inc., Washington, D.C., RTCA DO-294B, Dec. 13, 2006.

[5] "Radio Frequency Devices," Government Printing Office, Washington, D.C., Code of Federal Regulations Title 47 Part 15, Aug. 26, 2003.

[6] "Environmental Conditions and Test Procedures for Airborne Equipment," RTCA, Inc, Washington, D.C., DO-160D, July 29, 1997.

[7] H. Taub and D. L. Schilling, *Principles of Communication Systems*, 2nd ed. New York: McGraw-Hill, 1986.

[8] R. J. Kelly and D. R. Cusick, "Advances in Electronics and Electron Physics," vol. 68, P. Hawkes, Ed.: Academic Press, 1986.

[9] "Minimum Operational Performance Standards for Airborne ILS Localizer Receiving Equipment Operating Within the Radio Frequency Range of 108-112 MHz," RTCA, Washington, D.C., DO-195, 1986.

[10] E. F. C. LaBerge, "Derivation of Localizer Receiver Error Relations," Honeywell CST COE, Columbia, MD, CSTCOE-EFCL-0211A, February 7, 2005.

[11] E. F. C. LaBerge, "Link Budget Analysis of T-PED Interference to Localizer," Honeywell CSTCOE, Columbia, MD, CST/ACE-EFCL-0219A, Feb. 10, 2005.

[12] R. Frazier, R. J. Kelly, and T. Skidmore, "UWB RFI Protection Level for Avionics Receivers of the National Airspace System Operating Below One GHz (unpublished draft)," FAA Spectrum Office, Washington, D.C., Dec. 18., 2002.

[13] "VDL Mode 4 Airborne Architecture Study: Radio Frequency Interference Analysis," EUROCONTROL, Brussels, VM4AAS_D3.2_V7, 10 Dec, 2003.

REPORT DOCUMENTATION PAGE

Form Approved
OMB No. 0704-0188

1. REPORT DATE *(DD-MM-YYYY)*	2. REPORT TYPE	3. DATES COVERED *(From - To)*
01- 03 - 2007	Contractor Report	

4. TITLE AND SUBTITLE

An Analysis of the Effects of RFID Tags on Narrowband Navigation and Communication Receivers

5a. CONTRACT NUMBER

5b. GRANT NUMBER

5c. PROGRAM ELEMENT NUMBER

6. AUTHOR(S)

LaBerge, E. F. Charles

5d. PROJECT NUMBER

NNL06AC06P

5e. TASK NUMBER

5f. WORK UNIT NUMBER

23R-079-30-9D11-01

7. PERFORMING ORGANIZATION NAME(S) AND ADDRESS(ES)

NASA Langley Research Center
Hampton, VA 23681-2199

Honeywell Research and Technology Center
Columbia, MD 21046

8. PERFORMING ORGANIZATION REPORT NUMBER

NCCSRTC-EFCL-0261B2

9. SPONSORING/MONITORING AGENCY NAME(S) AND ADDRESS(ES)

National Aeronautics and Space Administration
Washington, DC 20546-0001

10. SPONSOR/MONITOR'S ACRONYM(S)

NASA

11. SPONSOR/MONITOR'S REPORT NUMBER(S)

NASA/CR-2007-214859

12. DISTRIBUTION/AVAILABILITY STATEMENT

Unclassified - Unlimited
Subject Category 04
Availability: NASA CASI (301) 621-0390

13. SUPPLEMENTARY NOTES

Langley Technical Monitor: Truong X. Nguyen
An electronic version can be found at http://ntrs.nasa.gov

14. ABSTRACT

The simulated effects of the Radio Frequency Identification (RFID) tag emissions on ILS Localizer and ILS Glide Slope functions match the analytical models developed in support of DO-294B provided that the measured peak power levels are adjusted for 1) peak-to-average power ratio, 2) effective duty cycle, and 3) spectrum analyzer measurement bandwidth. When these adjustments are made, simulated and theoretical results are in extraordinarily good agreement. The relationships hold over a large range of potential interference-to-desired signal power ratios, provided that the adjusted interference power is significantly higher than the sum of the receiver noise floor and the noise-like contributions of all other interference sources. When the duty-factor adjusted power spectral densities are applied in the evaluation process described in Section 6 of DO-294B , most narrowband guidance and communications radios performance parameters are unaffected by moderate levels of RFID interference. Specific conclusions and recommendations are provided.

15. SUBJECT TERMS

Interference; T-PEDs; RFID tags; Localizer; Glide Slope; ILS; Aeronautical Communications

16. SECURITY CLASSIFICATION OF:			17. LIMITATION OF ABSTRACT	18. NUMBER OF PAGES	19a. NAME OF RESPONSIBLE PERSON
a. REPORT	b. ABSTRACT	c. THIS PAGE			STI Help Desk (email: help@sti.nasa.gov)
					19b. TELEPHONE NUMBER *(Include area code)*
U	U	U	UU	38	(301) 621-0390